Res Chem Intermed (2017) 43:3163–3182
DOI 10.1007/s11164-016-2817-z

A novel nickel(II) complex obtained from 2-[(3-bromo-propylimino)-methyl]-phenol as a ligand: synthesis, structural characterization, electrochemical and electrocatalytical investigations

Ali Ourari[1] · Chahinaz Zoubeidi[1,2] · Wassila Derafa[1] · Sofiane Bouacida[3] · Hocine Merazig[3] · Emilia Morallon[4]

Received: 18 July 2016 / Accepted: 14 November 2016 / Published online: 29 November 2016

Abstract Herein, we describe the synthesis of novel bidentate Schiff base ligand 2-[(3-bromo-propylimino)-methyl]-phenol (HL) and its Ni(II) complex in 2:1 (ligand:metal) ratio. The synthesized ligand (HL) and its Ni(II) complex were characterized using routine spectroscopic techniques like microanalysis, UV–visible absorption spectroscopy, FT-IR, NMR (^{1}H and ^{13}C). A suitable single crystal of the nickel complex was obtained from acetone solution by slow evaporation and studied by X-ray diffraction to determine its molecular structure. The crystallographic data of the obtained Ni(II)-2L complex revealed that it possesses a monoclinic space group P 21/n with cell dimensions of $a = 10.6818(2)$ Å, $b = 7.1071(1)$ Å, $c = 13.7925(3)$ Å, $\beta = 105.51(1)°$, $Z = 4$. The electrochemical investigation of both ligand and its Ni(II)-2L complex was carried out by cyclic voltammetry. The cyclovoltammograms showed two redox systems, Ni(II)/Ni(I) and Ni(III)/Ni(II). Interestingly, it was revealed that the Ni(II)-2L complex can be polymerized into its poly-[Ni(II)-2L] films, and electrodeposited onto glassy carbon. The resulting Ni(II)/Ni(I) and Ni(III)/Ni(II) redox systems were advantageously used. The first

✉ Ali Ourari
alourari@yahoo.fr

✉ Wassila Derafa
soussou.derafa@yahoo.fr

[1] Laboratoire d'Electrochimie, d'Ingénierie Moléculaire et de Catalyse Redox (LEIMCR), Faculté de Technologie, Université Ferhat Abbas Sétif-1, Sétif 19000, Algeria

[2] Département Génie des Procédés, Faculté des Sciences Appliquées, Université Kasdi Merbah Ouargla, Ouargla 30000, Algeria

[3] Unité de Recherche de Chimie de l'Environnement et Moléculaire Structurale, Université Mentouri-Constantine, Constantine 25000, Algeria

[4] Departamento de Quimica Física and Instituto Universitario de Materiales, Universidad de Alicante, Apartado 99, 03080 Alicante, Spain

one was used in the electroreduction of bromocyclopentane while the second one Ni(III)/Ni(II) is rather applied to oxidize methanol.

Keywords Schiff base ligand · Ni(II) complex · X-ray diffraction · Cyclic voltammetry · Redox electrocatalytical properties

Introduction

The use of chelating agents in coordination chemistry such as Schiff base ligands having four (NNOO) donor atoms as in H_2Salen have been extensively studied in the literature [1–6]. In contrast, the similar structures with only two donor atoms commonly known as bidentate Schiff base ligands are generally less studied [7–9]. Due to this, a new class of ligands containing two donor sites of coordination with carbon–bromide function (C–Br) has attracted our attention because of their crucial role in chemical reactivity [4, 5]. These brominated or chlorinated precursors may play an important role in the synthesis of bidentate Schiff base ligands.

Owing to the electrophilic substitution reactions, the formation of new compounds containing electro-polymerizable entities such as anilinics, pyrrolics and thiophenics are of great interest [3, 10, 11]. Thus, these compounds could be used as new monomers to elaborate modified electrodes currently applied as materials useful in many domains as in catalysis [12], electrocatalysis [13–16] and in the detection of biomolecules as biosensors [17, 18]. This wide range of applications may also be extended to study the biological activities such as antibacterial [7, 19, 20], antifungal [8, 21], antitumoral activities [9], etc.

The above studies stimulated us to carry out the present work. Herein, we attempt to open new ways for the synthesis of Schiff base ligands with their corresponding complexes, especially those yielding new monomers (see Scheme 1). These various electropolymerizable monomers may be obtained from the considered starting material as depicted in Scheme 1.

In this paper, we describe a novel bidentate Schiff base nickel complex, derived from 3-bromopropyliminosalicylidene. The synthesized compounds were characterized by the routine spectral techniques such as UV–Vis, FT-IR, ^{1}H, ^{13}C NMR and X-ray diffraction. In addition, electrochemical study of the compounds and electropolymerization of monomers were performed by a cyclic voltammetry technique.

Experimental section

Materials

All the starting materials were obtained from commercial sources and were used as received without any further purification. For the cyclic voltammetry studies, dimethylformamide (DMF, 99.9%) was employed as the solvent, while tetra-*n*-butylammonium perchlorate (TBAClO_4, 98%) was used as the supporting

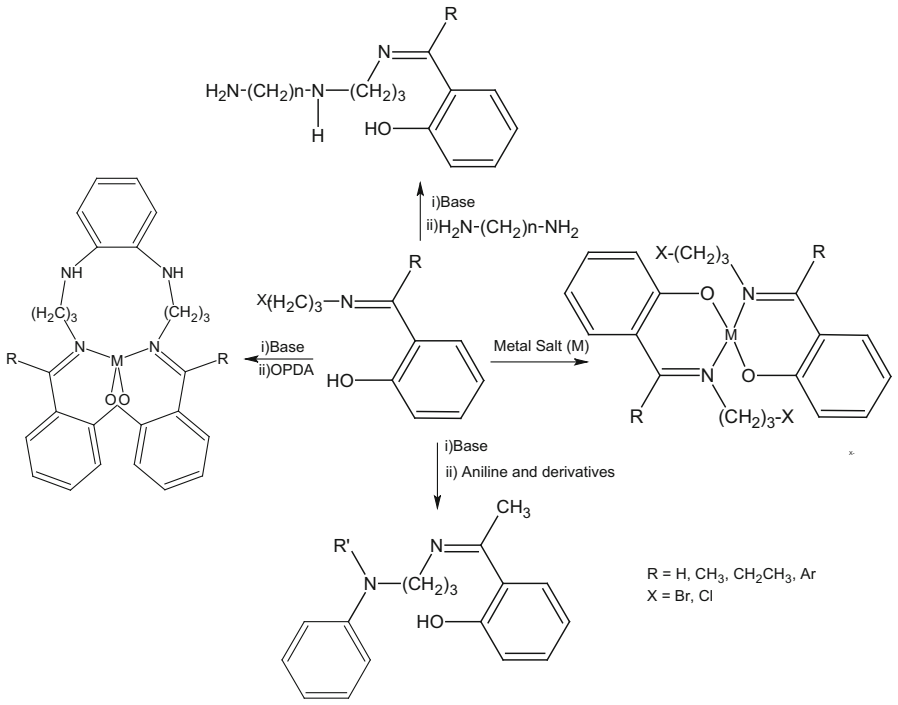

Scheme 1 Different reaction ways leading to new electropolymerizable monomers

electrolyte. This latter was recrystallized from water–methanol and thoroughly dried by continuous storage in a vacuum oven at 80 °C.

Physico-chemical characterization

The melting point of the synthesized product was recorded with the aid of a Kofler bench apparatus. ^{1}H nuclear magnetic resonnce (NMR) and ^{13}C–{^{1}H} NMR spectra were obtained on a BRUKER AVANCE DPX 250 MHz spectrometer. Fourier transform infrared (FT-IR) spectra (KBr, 4000–500 cm^{-1}) were recorded using a Perkin–Elmer RXI spectrometer. Electronic spectra were recorded on a Shimadzu UV-1800 spectrophotometer using ethanol and dimethylformamide as solvents. The scanning electron microscopy (SEM) was carried out on a JEOL 2600F with a resolution of 5 nm. The sample was deposited onto a double-face graphite tape in order to avoid a charging effect during the analysis.

X-ray diffraction

A single crystal of the studied complex, Ni(II)-2L, with dimensions of 0.11 × 0.12 × 0.15 mm3, was selected for single crystal X-ray diffraction analysis. Data collection was performed at 295(2) K on a Bruker APEXII diffractometer,

charge-coupled device (CCD) area detector equipped with a graphite monochromatized MoKα radiation ($\lambda = 0.71073$ Å).

The reported structure was solved by direct methods with SIR2002 [22] to locate all the non-H atoms which were refined anisotropically with SHELXL97 [23] using a full-matrix least-squares on F^2 procedure from within the WinGX [24] suite of software used to prepare material for publication. All the H atoms were placed in the calculated positions and constrained to ride on their parent atoms.

Electrochemical study of Ni(II)-2L complex behavior

The electrochemical study of Ni(II)-2L nickel complex was carried out at room temperature (~25 °C) by cyclic voltammetry using a mono-compartment cell with 5 mL as capacity. The conventional three-electrode system was adopted to perform all the experiments in acetonitrile solutions (CH_3CN) containing 0.1 M tetra-*n*-butylammonium perchlorate (TBAP) and 0.001 M of the complex. The working electrode was a disc of glassy carbon (GC; diameter of 3 mm) while the counter electrode was a platinum wire, and the reference was a saturated calomel electrode (SCE). The GC electrodes were polished by diamond paste and copiously rinsed with acetone and then acetonitrile. The modified electrodes were characterized by cyclic voltammetry using a standard set-up.

Chemistry

Synthesis of (2-{(E)-[3-bromopropyl)imino]methyl}phenol (HL)

To an ethanolic solution of 2-hydroxybenzaldehyde, a solution of 3-bromopropylammonium hydrobromide in absolute ethanol (15 mL) was added at an 1:1 molar ratio. 0.5 mMol of sodium carbonate (Na_2CO_3) was added and the resulting mixture was refluxed under nitrogen atmosphere for 2 h at 60 °C [25]. The expected compound was extracted by dichloromethane, dried with anhydrous sodium sulfate and, then, yellow viscous oil was recovered after elimination of the solvent under reduced pressure using a rotary evaporator.

Yield 82%. UV–Vis, λ_{max} (nm) (ε_{max} ($dm^3\ mol^{-1}\ cm^{-1}$)) (ethanol): 320 (4.8×10^4), 254 (1.5×10^4). FT-IR (KBr pellet, cm^{-1}): $\nu_{C–OH}$ centered at 3420 (broad), $\nu_{C–Harom.}$ 3092 (w), 3015 (w), $\nu_{CH_2\,aiph(asym)}$ 2922 (m), $\nu_{CH_2\,aiph(sym)}$ 2850 (m), $\nu_{C=N}$ 1635 (s), 1541(s), 1475 (m), 1456 (m), 667 (m), 534 (s). ^{1}H NMR ($CDCl_3$, 25 °C, 250.13 MHz, ppm): δ 13.42 (s, 1H, O–H), 8.45 (s, 1H, H–CN), 7.10–7.40 (m, 4H, Ph), 3.87 (t, 2H, CH_2Br), 3.59 (t, 2H, N–CH_2), 2.32 (m, 2H, N–CH_2–CH_2–CH_2Br. ^{13}C NMR ($CDCl_3$, 25 °C, 68.70 MHz, ppm): δ 31.275 (CH_2Br), 33.095 (–CH_2–), 57.215 (NCH_2), 117.113, 118.847, 131.512, 132.526, 161.625 (C=C, Ph), 166.970 (CN).

Synthesis of nickel Schiff base complex (Ni(II)-2L)

0.5 mMol of nickel acetate tetrahydrate was dissolved in 5 mL of absolute ethanol and added to an ethanolic solution containing 1.0 mMol of ligand HL. This mixture

was refluxed under stirring and nitrogen atmosphere for 2 h at 60 °C. The obtained precipitate was filtered, washed with cold ethanol and then dried in oven at moderate temperature. The suitable single crystals were obtained from acetone solution by slow evaporation yielding bright green single crystals.

Yield 72%. Melting point: 160 °C. UV–Vis, λ_{max} (nm) (ε_{max} ($dm^3\ mol^{-1}\ cm^{-1}$)) (ethanol) = 619 (2.3×10^3), 419 (1.336×10^5), 329 (2.593×10^5), 268 (1.5×10^5). FT-IR (KBr pellet, cm^{-1}): $\nu_{C–Harom.}$ 3092 (w), $\nu_{C–Harom.}$ 3015 (w), $\nu_{CH_2\,aiph(asym)}$ 2923 (m), $\nu_{CH_2\,aiph(sym)}$ 2853 (m), 1607 (s), 1544 (m), 1450 (m), 1333 (s), 1042 (w), 717 (m), 568 (s), 534 (m), 521 (w), 498 (w).

Results and discussion

Synthesis

The ligand HL was prepared by reacting 3-bromopropyl ammonium hydrobromide with 2-hydroxybenzaldehyde at a 1:1 M ratio in the presence of a base in absolute ethanol to activate the nucleophilic character of the amino group (–NH_2). The ligand is soluble in all common organic solvents. The synthesis of Ni(II)-2L complex was achieved by refluxing the ligand HL with nickel(II) acetate tetrahydrate in absolute ethanol. The reaction pathways leading to the formation of the ligand (HL) and its Ni(II)-2L complex are illustrated in the following Scheme 2.

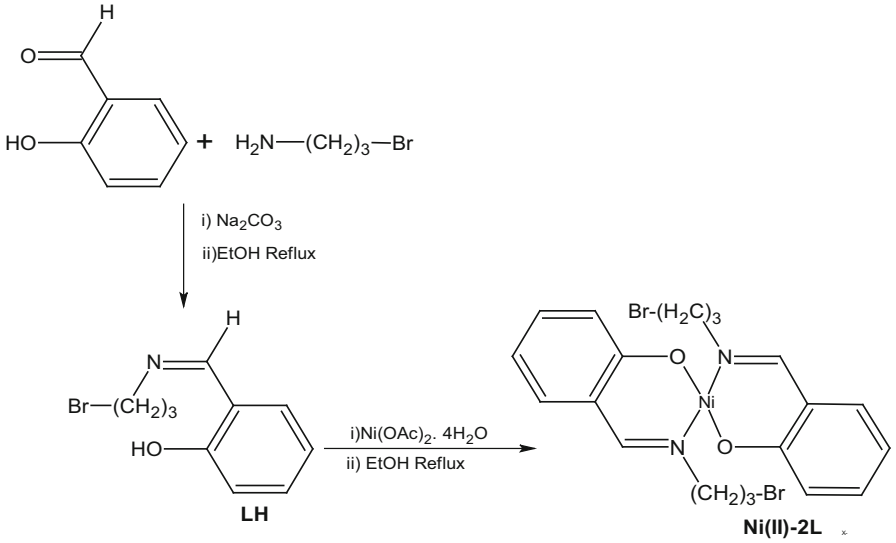

Scheme 2 Synthesis of new bidentate (NO) Schiff base ligand (HL) and its nickel(II) Schiff base complex (Ni(II)-2L)

UV–Vis spectrophotometry

Typical absorption peaks of aromatic moieties were observed for the ligand (HL) and its Ni(II)-2L complex. The ligand shows two absorption peaks at 254 and 320 nm whereas its corresponding Ni(II)-2L complex exhibits four peaks at 268, 329, 419 and 619 nm. In both cases, the first band corresponds to phenyl-ring $\pi \rightarrow \pi^*$ electronic transitions [26] while the second peak was assigned to $n \rightarrow \pi^*$ transition of the aromatic moiety of the ligand [27]. As for the third peak observed at 419 nm it was ascribed to the Soret band [27], suggesting that the nickel(II) ion is effectively coordinated to the ligand [28, 29]. The fourth peak located at 619 nm was attributed to the d–d electronic transitions which are generally known by their weaker intensities [10, 11].

FT-IR spectrophotometry

The IR spectrum of the ligand exhibits a broad absorption band in the region 3300–3600 cm^{-1} that can be assigned to intra- and inter-molecular hydrogen bonds arising from the presence of hydroxyl groups (phenol). The ν_{C-H} aromatic frequencies appeared at 3090, 3010 cm^{-1} while the absorption bands of ν_{CH_2} aliphatics such as $\nu_{CH_2(as)}$ non-symmetrical and $\nu_{CH_2(s)}$ symmetrical were also observed at 2922 and 2850 cm^{-1}, respectively. Absorption bands appearing at 1635 cm^{-1} are attributed to $\nu_{C=N}$ stretching vibrations whereas the frequencies of the $\nu_{C=C}$ aromatic double bonds were seen as two or three peaks around 1550 and 1450 cm^{-1}. As for the ν_{C-O} absorption bands, they were also depicted around 1215 cm^{-1}. For the ν_{C-H} bands of bending out of plane, they were found at 667 cm^{-1} and those of CH_2–Br moieties at 534 cm^{-1}. The IR spectrum of the Ni(II)-2L complex shows a neat shifting of an azomethine group to the lower frequencies, when compared to its equivalent absorption bands observed for the ligand at 1635 cm^{-1}. The frequency of the azomethine group is located at 1607 cm^{-1}. This shifting $\Delta\nu$ estimated to 28 cm^{-1} may be explained by a significant extension of the electronic delocalization through the transition metal (Ni). This is also supported by an indication suggesting that the azomethine group is effectively coordinated to the metal center of Ni(II)-2L complex [30–32]. Inversely, the (C–O) absorption band shifts to higher wave numbers from about to 1215 to 1333 cm^{-1} expressing a strengthening of the electronic density for the C–O bond after its coordination to the metallic center [31]. These two observations are due to the coordination of metallic cation through the oxygen atoms of ionized hydroxyl groups and the nitrogen atoms of azomethine groups [26, 27]. In addition, other new bands observed at 498 and 521 cm^{-1} confirm the nature of the metal–ligand bonding appearing at lower energy and they are assigned to Ni(II)–N and Ni(II)–O vibrations, respectively [33, 34].

NMR spectra

The ^{1}H NMR spectrum of HL ligand reveals a downfield singlet signal at 13.62 ppm which is ascribed to the phenolic proton. Aromatic protons of the ligand appear as a

complex multiplet between 7.10 and 7.40 ppm, centered at 7.25 ppm. As for the **CH_2**–Br moiety resonating as a triplet, it was observed at 3.59 ppm due to the electronegativity of the bromine atom whereas the methylene group attached to the imine group **CH_2**–N=C appears at 3.87 ppm. The methylene group between the two previous methylene groups $(–CH_2–)_n$ was observed as a quintuplet at 2.32 ppm. The proton linked to the imine function, i.e., N=CH, resonates as a singlet at 8.45 ppm as currently observed for this kind of compound. These results are in good agreement with those described in the literature for compounds showing similar structures [30, 31, 35].

In the ^{13}C NMR spectrum of the ligand, each one of the different carbon resonances appears at its characteristic zone according their own typical hybridization. For the carbon atoms, resonations at 117–161 ppm are associated with sp2 hybridized aromatic carbons. The carbon atom of the azomethine group is observed at 162.40 ppm whereas sp3 hybridized aliphatic carbon atoms resonate in the 31–57-ppm range. Carbon atoms such as Br–**CH_2**, Br–CH_2–**CH_2**–CH_2–N=CH and **CH_2–N**=CH were observed at 31.275, 33.095, and 57.215 ppm, respectively. It can also be concluded that the results obtained are in good accordance with those reported in the literature [33–35].

Crystal and molecular structure of the Ni(II)-2L

According to single crystal X-ray structure analysis, an ORTEP view of the Ni(II)-2L complex with atoms numbering is given in Fig. 1. Table 1 lists selected bond

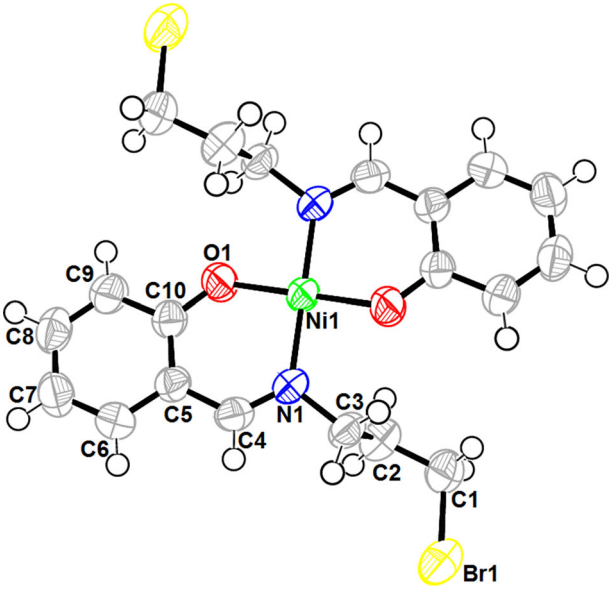

Fig. 1 An ORTEP view of Ni(II)-2L Schiff base complex with an atomic labelling scheme. Displacement is drawn at the 50% probability level. Only the contents of the asymmetric unit are numbered

Table 1 Select bond distances/Å and bond angles/° for Ni(II)-2L

Ni1–O1^{i}	1.8268 (13)	O1^{i}–Ni1–N1	87.11 (6)
Ni1–O1	1.8268 (13)	O1–Ni1–N1	92.89 (6)
Ni1–N1	1.9274 (15)	O1^{i}–Ni1–N1^{i}	92.89 (6)
Ni1–N1^{i}	1.9274 (15)	O1–Ni1–N1^{i}	87.11 (6)
O1^{i}–Ni1–O1	180.0000 (10)	N1–Ni1–N1^{i}	180.0000 (10)

Symmetry code: ^{i} $-x + 2, -y, -z + 2$

lengths and angles. Structural resolution revealed that the Ni atom is located at an inversion centre. The Ni(II) ion is coordinated by two nitrogen and two oxygen atoms of two independent bidentate ligands in the basal plane and by one oxygen atom in the apical position.

In this complex, the Schiff base ligand exhibits an anionic form with N and O atoms as a bidentate ligand. The Ni–O and Ni–N bond lengths are 1.8268 and 1.9274 Å, respectively (See Table 1).

Selected bond lengths (Å) and bond angles (°) are; Ni1–N1 1.8268 (13), Ni1–O01 1.9274 (15) O01–Ni1–N1 87.11 (6), N1–Ni1–O 01 92.89 (6).

The crystallographic data and experimental details for structural analysis are summarized in Table 2.

Electrochemical characterization

Cyclic voltammetry of the ligand and its nickel complex

The electrochemical behavior of a GC electrode freshly polished in 1 mM solution of the ligand and 1 mM of the nickel complex was studied in acetonitrile solution under argon atmosphere and containing 0.1 M TBAP. The voltammograms were recorded at 100 mV s^{-1}.

Figure 2 shows the voltammograms of the ligand (black line) during the first cycles in which two oxidation peaks are observed in more positive potentials, observed at $Epa_2 = 1.612$ and $Epa_3 = 1.101$ V/SCE; they can be attributed to the oxidation of the phenolic group with its ortho- and para- positions, respectively [31, 36]. These peaks show the counterparts at $Epc_1 = 1.352$ and $Epc_2 = 0.714$ V/SCE during the reverse scan. At less positive potentials, a reduction peak located at $Epa_1 = -1.797$ V/SCE is assigned to the reduction of the azomethine groups [37, 38].

As for the nickel complex, its voltammetric behavior is also shown in Fig. 2. At more positive potentials, three oxidations peaks can be observed at $Epa_3 = 0.894$, $Epa_4 = 1.166$ and $Epa_5 = 1.683$ V/SCE. The first one may be associated with the oxidation of Ni(II) to Ni(III) species and to the oxidation of the phenolic moieties, respectively. The peaks at more negative potentials at $Epa_1 = -1.378$ and $Epa_2 = -0.800$ could be as well associated with the reduction of the azomethine groups and to the oxidation of the Ni(I) to Ni(II) species.

Table 2 Crystallographic and structural refinement data for Ni(II)-2L

CCDC deposition number	1044698
Empirical formula	C20 H22 Br2 N2 CuO2
Formula weight	545.75
T (K)	295
λ (Å)	0.71073
Crystal system	Monoclinic
Space group	P 2_1/n
Unit cell dimensions (Å, °)	
a (Å)	10.6478 (4)
b (Å)	7.1990 (3)
c (Å)	13.9283 (5) A
α (°)	90
β (°)	104.900 (2) °
γ (°)	90
Volume (Å^3), *Z*	1031.75 (7), 2
Calculated density (g cm^{-3})	1.757 Mg m − 3
Absorption coefficient (mm^{-1})	4.95
F (000)	542.0
θ range for data collection(°)	3.2–27.7
Limiting indices	*h*: −12/14
	k: −9/6
	l: −18/18
Data/restraints	3050/0
Parameters	124
Total reflections	11,826
Unique reflections (Rint)	3050 (0.0243)
Completeness	0.998
Refinement method	Full least-squared (Shelxl)
Goodness-of-fit on F^2	1.04
Final R index [I > 2σ(I)]	0.032
R index [all data]	0.089
Largest difference peak and hole (e Å^{-3})	0.62/−0.58

In this last case, it can be noted that this reduction wave was significantly shifted to the less cathodic potentials with respect to the ligand compound. This shifting to the potential values was explained by a decrease of the electron density of the imine group after formation of the nickel complex by coordination linking [38, 39].

Figure 3a shows a pair of oxidation–reduction peaks corresponding to the Ni(III)/Ni(II) redox couple for which $Epa_3 = 0.930$ and $Epc_3 = 0.624$ V/SCE lead to an average formal potential $E_{1/2} = 0.794$ V/SCE. The peak to peak separation between the anodic and cathodic potentials is $\Delta Ep_1 = 0.306$ V. The ratio of the peak currents (Ipc_3/Ipa_3) was found to be higher than unity (1.51). Figure 3b exhibits the

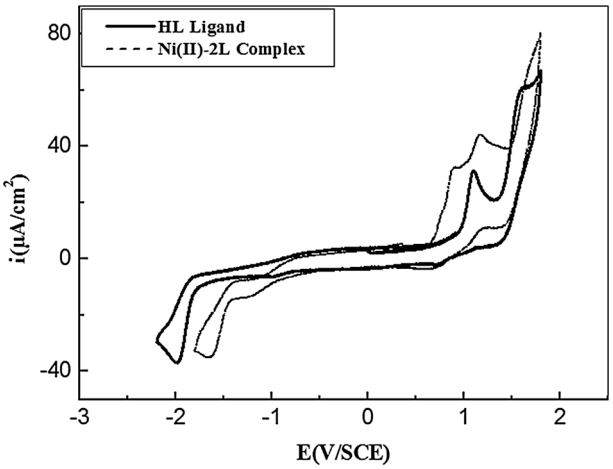

Fig. 2 Cyclovoltammograms of 1 mM of HL (*full line*), 1 mM of Ni(II)-2L (*dashed line*), 10^{-1} M TBAP, acetonitrile solutions, 100 mV s^{-1} as scan rate

electrochemical behavior of the Ni(II)/Ni(I) redox couple for which $Epa_2 = -1.150$ and $Epc_2 = -0.620$ V/SCE. The peak to peak separation ΔEp_2 between anodic and cathodic waves was estimated to be 0.392 V. In this case, it was also noted that the ratio of the both peak currents Ipa_2/Ipc_2 is again higher than unity (1.84). These two redox couples seem to be irreversible since the results obtained may approach those reported by the literature [37, 40, 41].

Figure 3a shows that the Ni(III)/Ni(II) redox couple seems to be dependent on the scan rates, especially for the anodic wave. This anodic wave, at low rates (10–100 mV s^{-1}), splits in two waves $Epa_{(I)}$ and $Epa_{(II)}$ becoming at higher scan rate $\geq$100 mV s^{-1} a unique wave. Here, it was observed that as the scan increases, both waves $Epa_{(I)}$ and $Epc_{(II)}$ shift to more anodic and cathodic potentials, respectively. An increase in peak currents was also noted [5, 39]. Figure 3b exhibits a pair of oxidation–reduction waves of Ni(II)/Ni(I) demonstrating a similar behavior, as was observed earlier for the Ni(III)/Ni(II) redox system [41].

Electropolymerization of Ni(II)-2L complex onto GC and indium tin oxide (ITO) electrodes

Nickel(II) complex was electropolymerized on a GC electrode during anodic oxidation by cycling between 0.0 V to 1.200 V/SCE (Fig. 4a). The continuous increase in the (*ipa*, *ipc*) peak currents with the number of cycles was observed at around 0.65 V/SCE, as above noted for Fig. 4a. Therefore, the same figure indicates the formation of a polymeric film on the electrode surface. This electropolymerization reaction was carried out in 0.1 M TBAP/CH_3CN using 1.0 mM as the concentration of monomer Ni(II)-2L complex and its poly-Ni(II)-2L films effectively obtained.

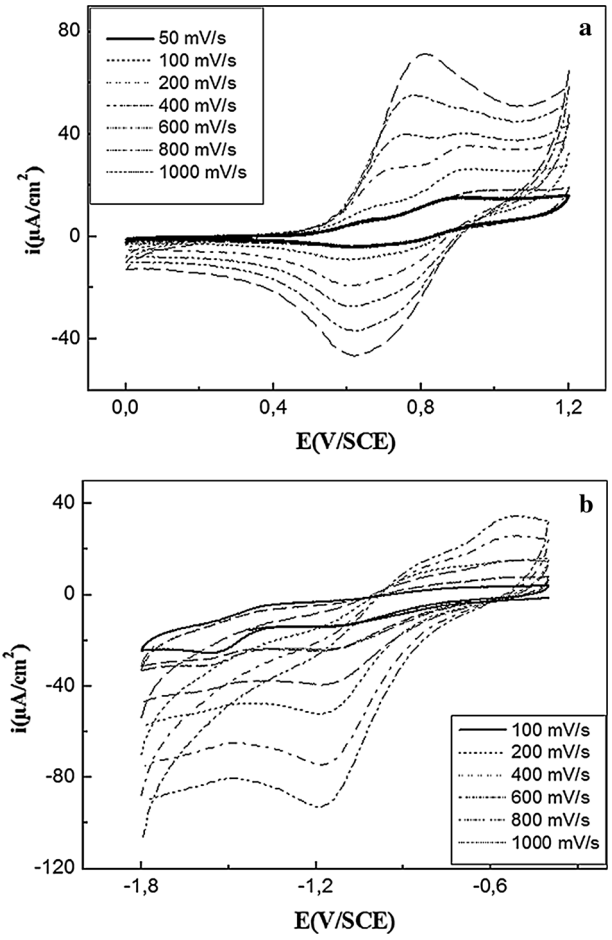

Fig. 3 Cyclovoltammograms showing scan rate dependence: **a** Ni(II)/Ni(III) redox couple, 1 mM of Ni(II)-2L, 0.1 M TBAP/CH_3CN, **b** Ni(I)/Ni(II) redox couple, 1 mM of Ni(II)-2L, 0.1 M TBAP/CH_3CN

The behavior of the Ni(II)/Ni(III) redox couple shows a continuous increasing of its anodic and cathodic (*ipa* and *ipc*) peak currents with the increase of the cycle number. This increase of *ipa* and *ipc* is accompanied by a shifting of the peak potentials (See Fig. 4a) [17, 42, 43].

On the cathodic sweep, the same Ni(II)-2L complex is also involved in the preparation of another modified GC electrode with recording of the Ni(II)/Ni(I) redox couple. Also, the poly-(Ni(II)-2L) films were electrodeposited by a cycling technique between −0.400 and −1.800 V/SCE [17] (See Fig. 4b). For this redox couple, the modified electrode was prepared with only 30 cycles. Figure 4b shows the evolution of the cyclovoltammograms of Ni(II)-2L complex during repeated potential scans as previously indicated. The continuous increase in the peak current *(ipa* and *ipc*) amplitudes of Ni(II)/Ni(I) indicates the formation of polymeric films at the electrode surface. The increase of cycle number causes not

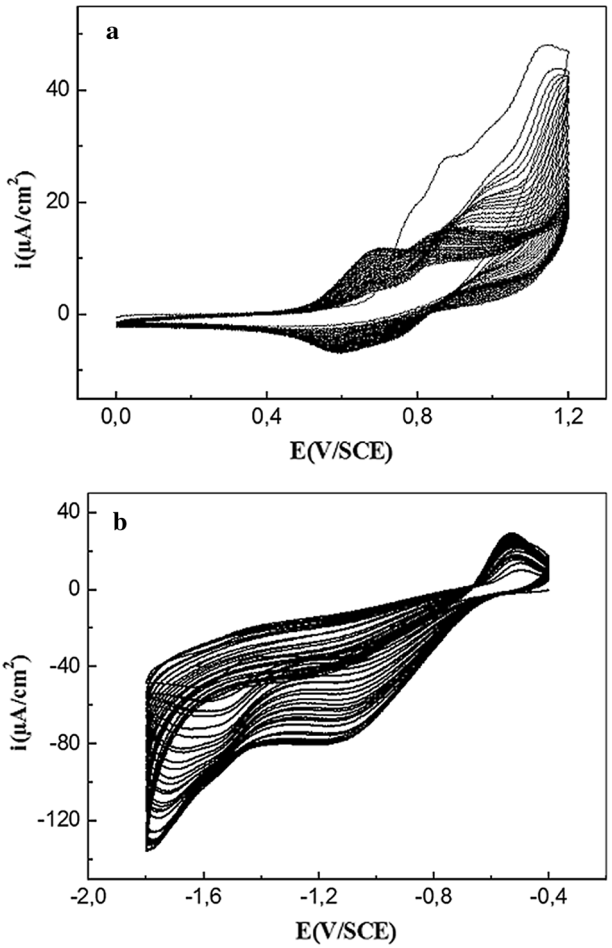

Fig. 4 **a** Electropolymerization of 0.01 M of Ni(II)-2L, 0.1 M TBAP/CH_3CN by cycling between 0.0 and 1.2 V/SCE at 100 mV s^{-1} using a GC electrode (50 cycles). **b** Cathodic electropolymerization of 0.01 M of Ni(II)-2L, 0.1 M TBAP/CH_3CN by cycling between −0.4 and −1.8 V/SCE at 75 mV s^{-1} using a GC electrode (30 cycles)

only an increase of peak current value, but also a displacement of the potential to more negative values. The Audebert group and other authors [44–46] proposed that the oxidative polymerization of nickel Schiff-base complexes is essentially produced on the ligand structure, based on the stabilizing cation radical inducing radical–radical coupling between the para-phenol rings which are responsible for polymer formation. This new material may also be considered as another modified electrode.

This electropolymerization process was also carried out according the same manner with nickel(II) complex to obtain its poly-(Ni(II)-2L) films, electrodeposited onto the ITO electrode surface, as was illustrated by the following Fig. 5.

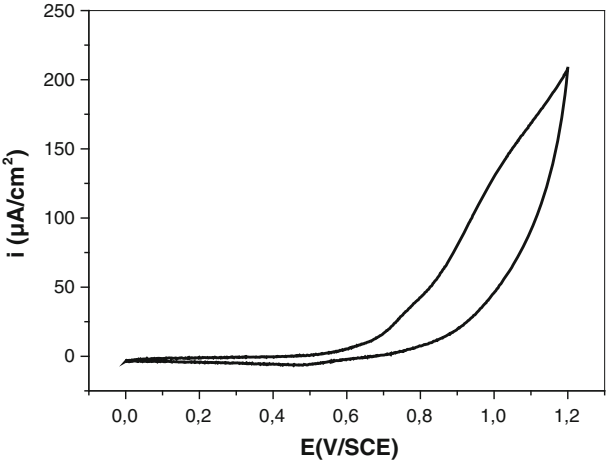

Fig. 5 Cyclovoltamogram recorded with a poly-Ni(II)-2L/GC modified electrode after its transfer in fresh 0.1 M TBAP/CH_3CN solution using 50 mV s^{-1} as the scan rate

Morphological characterization with SEM

Figure 6 shows a typical scanning electron micrograph of the poly[Ni(II)-2L] films electrodeposited onto an ITO substrate surface as modified electrodes by successive cycling in the potential values ranging from 0 to 1200 V/SCE. As it is clearly seen in Fig. 6, the poly[nickel(II)-complex] films show the presence of microparticles on the surface onto the ITO electrode surface with most particles (Fig. 6e, f). Figure 6b exhibits obviously as well an heterogeneous distribution of poly[Ni(II)-2L] films as particles obtained during this electropolymerization process [14].

Analysis of the ITO electrode surface by XPS

X-ray photoelectron spectroscopy (XPS) was used to examine the surface composition of Ni(II)-2L/ITO. Based on these analyses, nickel is present approximately at the different ratio in Ni(II)-2L and poly Ni(II)-2L. Also, it can be observed in its various forms (Ni free and poly-Ni). Some kinetic energy shifts were observed for poly Ni(II)-2L (Fig. 7a) when comparing to free nickel Ni(II)—Fig. 7b; XPS.

Figure 7a, b, given below, shows wide-scan X-ray photoelectron spectra of Ni(II)-2L and poly-Ni(II)-2L/ITO films as modified electrodes. The Ni coverage is clearly higher in Ni(II)-2L than in poly-Ni(II)-2L films/ITO. The spectrum of the poly-Ni(II)-2L films/ITO sample shows large C 1s and Cl 2p contributions, with weak Ni p and Ni Auger signals also being apparent. This indicates that the electrode surface is covered by a layer of Ni(II)-2L oxidation products. In agreement with this, no contribution from the ITO substrate was noted. The narrow-scan Ni 2p spectra of the above-mentioned samples (Fig. 7a, b) show the main Ni

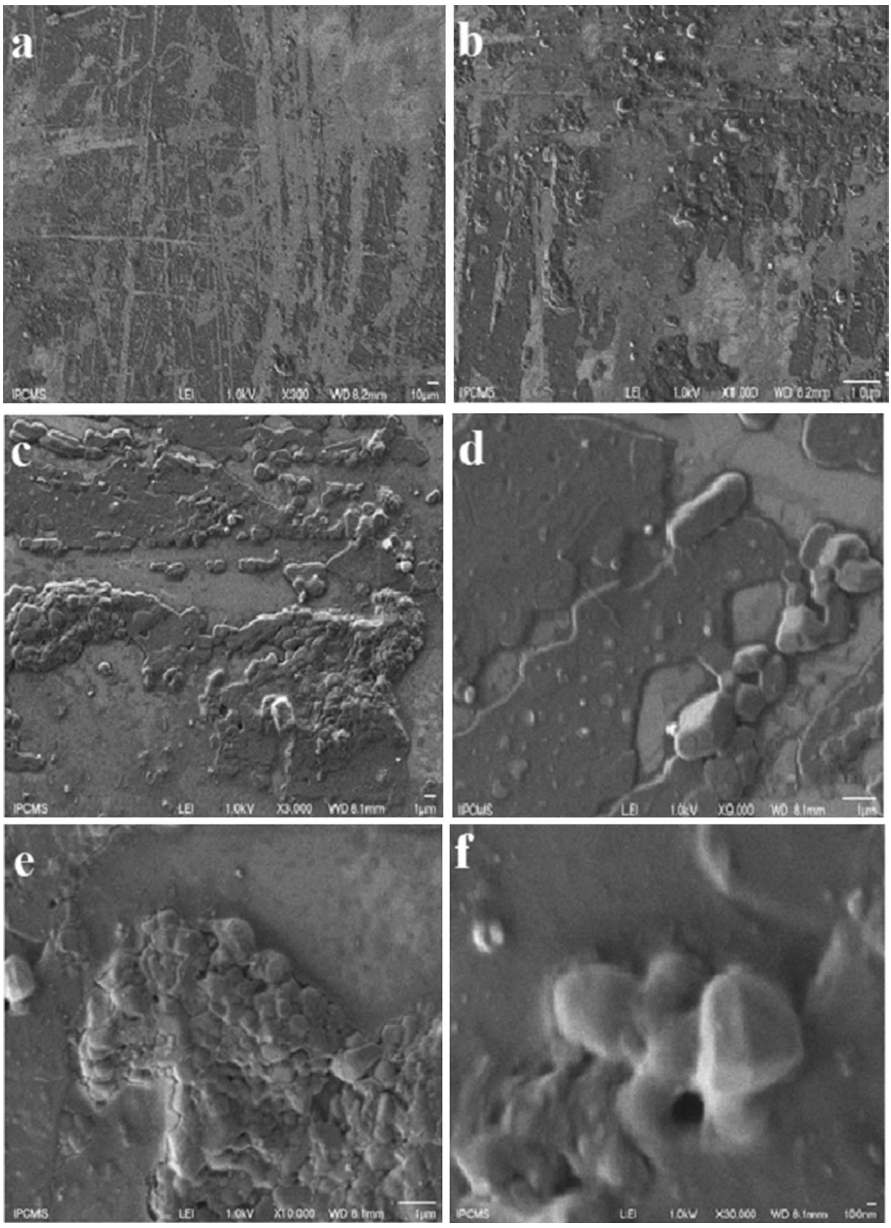

Fig. 6 Scanning electron micrographs of the ITO modified electrode surface with poly Ni(II)-L_2, **a** (X300, 1.0 kV 1 μm), **b** (X1.000, 1.0 kV 1 μm), **c** (X3000, 1.0 kV 1 μm), **d** (X9.000, 1.0 kV 1 μm), **e** (X10.000, 1.0 kV 1 μm), **f** (X30.000, 1.0 kV 100 nm)

$2p_{3/2}$ and Ni $2p_{1/2}$ signals appearing at 856.5 and 874.1 eV, respectively [14, 50]. The essential results obtained by this analysis are summarized in the following Table 3.

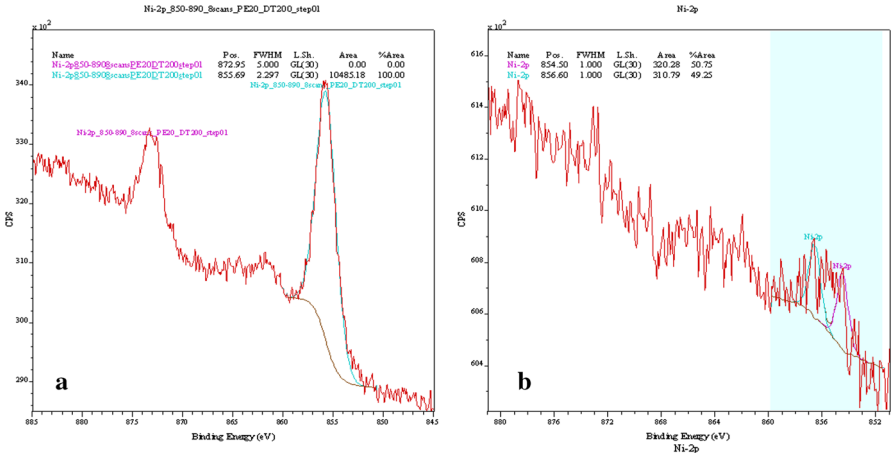

Fig. 7 XPS analysis of nickel 2p electron binding energies in: **a** Ni(II)-2L complex powder and **b** poly-Ni(II)-2L films electrodeposited onto the ITO surface

Table 3 Quantitative element distribution in atomic percentage determined from XPS analysis of the polyNi(II)-2L films/ITO modified electrode

Material	Surface concentration (at%)					Binding energy (eV)	
	C	N	O	Br	Ni	N	Ni
Ni(II)-2L	77.14	3.96	10.97	6.50	1.39	399.01, 400.0	855.69, 872.95
PolyNi(II)-2L/ITO	84.34	1.81	9.26	4.52	0.04	399.01, 400.56	854.50, 856.56

Electrocatalytical properties

Electrocatalytical oxidation of methanol

Figure 8 shows the electrochemical oxidation of methanol on unmodified GC and modified GC electrodes by electrodeposited poly-Ni(II)-L films. The electrochemical oxidation of methanol with the unmodified GC electrode appears to be poor, whereas the GC electrode modified by electrodeposition of poly-Ni(II)-L films onto its surface shows clearly an increase in the oxidation peak current expressing the oxidation reaction of methanol, attesting to the presence of a catalytic effect obtained from the polymer film containing catalytic sites such as Ni(II)-L complex molecules in their solid phase immersed in 0.1 M TBAP/CH_3CN solution. Thus, this illustrates clearly the dependence of methanol on the electro-oxidation peak currents as can be seen in Fig. 8. The voltammograms, recorded during the positive sweep using the poly-(Ni(II)-2L) films, proved that the electrocatalytic oxidation reaction is obviously dependent on the methanol concentration. The oxidation peak

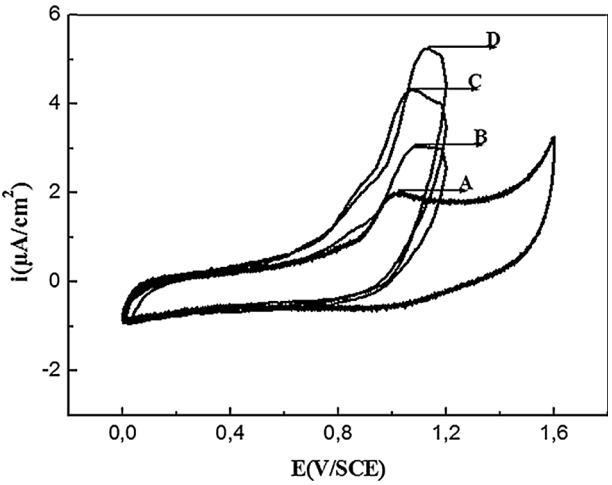

Fig. 8 Cyclovoltammograms recorded in 0.1 M TBAP/CH_3CN solutions using 100 mV/s as the scan rate: **a** GC electrodes in the presence of 1 mM of methanol, poly-Ni(II)-2L/GC modified electrode; **b** in the absence of methanol; **c**: 0.25, **d** 1 mM of methanol

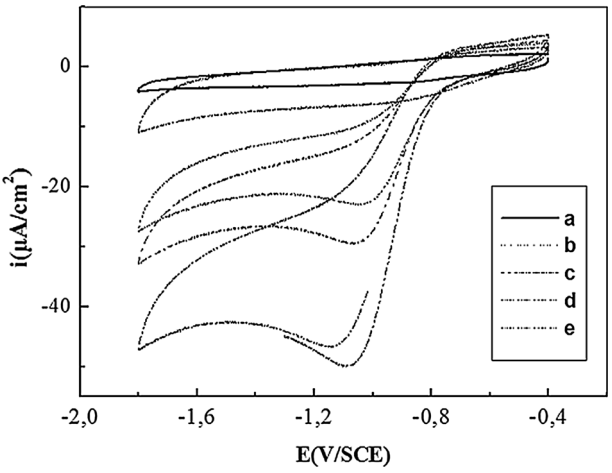

Fig. 9 Cyclovoltammograms recorded in 0.1 M TBAP/CH_3CN solutions using 100 mV/s as the scan rate: **a** GC electrodes, poly-Ni(II)-2L/GC modified electrode: **b** 0 mM, **c** 2.0 mM, **d** 4.0 mM, and **e** 10.0 mM of bromocyclopentane

current, at higher methanol concentrations, increases at first, but then its growth starts to level off [47, 48].

Electrocatalytical reduction of bromocyclopentane

Electrochemical reduction of bromocyclopentane was also studied on a GC electrode modified with Ni(II)-2L polymer film, in 0.1 M TBAP/CH_3CN solution

from 0 to −1.200 V/SCE using 100 mVs^{-1} in the presence and absence of bromocyclopentane. In the absence of bromocyclopentane (Fig. 9, curve b), the irreversible one-electron nickel(II)–nickel(I) process is observed as previously indicated. The reduction of bromocyclopentane by the modified electrode (Fig. 9) was observed in −1.040 V/SCE, which can be assigned to bromocyclopentane reduction where the Ni(II)/Ni(I) redox system is involved. When bromocyclopentane is added to this electrocatalytic system (Fig. 9, curves c–e), a reduction peak was clearly observed at −1.05 V which increases with the concentration of bromocyclopentane. Thus, nickel(I) species catalyze the reduction of the bromocyclopentane because of the progressive disappearance of the anodic peak involved in the Ni(II)/Ni(I) redox system. The electrochemical reduction of bromocyclopentane using modified GC electrodes has been recently discussed [3, 49].

Conclusion

In summary, the synthesis and characterization of bidentate Schiff base ligand (N-3-bromopropylsalicylaldimine) and its corresponding nickel(II) complex were synthesized and characterized with various spectral techniques. The obtained complex behaves as a monomer, since it was easily electropolymerized onto ITO and GC substrates, leading to the formation a modified electrode by oxidation/reduction processes. The morphologies of the modified electrode surfaces were explored by scanning electronic microscopy (SEM) and their content was analyzed by an XPS technique. Two redox systems, Ni(II)/Ni(I) and Ni(III)/Ni(II), characterizing the metallic center such as nickel, were found to be irreversible. The good electrocatalytical activity of this new material has been demonstrated by cyclic voltammetry using electro-oxidation of methanol and electroreduction of bromocyclopentane. Work is now in progress in our laboratory to synthesize many other new electrode materials.

Acknowledgements The authors thank the Algerian « Ministère de l'Enseignement Supérieur et de la Recherche Scientifique et la Direction Générale de la Recherche » for financial support. The authors would like also to thank the laboratory of CNRS (ICPEES - UMR 7515) of Strasbourg university for its valuable helping.

References

1. A. Burkhardt, H. Görls, W. Plass, Nickel(II) complexes with Schiff-base ligands derived from epimeric pyranose backbones as 2,3-chelators: modeling the coordination chemistry of chitosan. Carbohydr. Res. **343**, 1266–1277 (2008)
2. J.W. Lu, Y.H. Huang, S.I. Lo, H.H. Wei, New μ-oxo-bridged tetranuclearCu(II) complex with Schiff-base ligand: synthesis, crystal structure and magnetic properties. In. Chem. Commun. **10**, 1210–1213 (2007)
3. A. Ourari, Y. Ouennoughi, D. Aggoun, M.S. Mubarak, E.R. Pasciak, D.G. Peters, Synthesis, characterization and electrochemical study of new tetradentate nickel(II)-Schiff base complex derived from ethylendiamine and 5′-(N-methyl-N-phenylaminomethyl)-2′-hydroxyacetophenone. Polyhedron **67**, 59–64 (2014)

4. S. Saha, R.K. Kottalanka, P. Bhowmik, S. Jana, K. Harms, T.K. Panda, S. Chattopadhyay, H.P. Nayek, Synthesis and characterization of a nickel(II) complex of 9-methoxy-2,3-dihydro-1,4-benzoxyzepine derived from a Schiff base ligand and its ligand substitution reaction. J. Mol. Struct. **2014**, 26–31 (1061)
5. I.C. Santos, M. Vilas-Boas, M.F.M. Piedade, C. Freire, M.T. Duarte, B. de Castro, Electrochemical and X-ray studies of nickel(II) Schiff base complexes derived from salicylaldéhyde; Structural effects of bridge substituents on the stabilisation of theq3 oxidation state. Polyhedron **19**, 655–664 (2000)
6. J. Tisato, F. Refosco, F. Bandoli, Structural survey of technetium complexes. Coord. Chem. Rev. **135**, 325–397 (1994)
7. J. Devi, N. Batra, Synthesis, characterization, antifungal, antibacterial and DNA cleavage studies of some heterocyclic Schiff base metal complexes. Spectroc. Acta A **135**, 710–719 (2015)
8. S.A. Patil, C.T. Prabhakara, B.M. Halasangi, S.S. Toragalmath, P.S. Badami, DNA cleavage, antibacterial, antifungal and anthelmintic studies of Co(II), Ni(II) and Cu(II) complexes of coumarin Schiff bases: synthesis and spectral approach. Spectroc. Acta A **137**, 641–651 (2015)
9. M. El-Behery, H. El-Twigry, Synthesis, magnetic, spectral, and antimicrobial studies of Cu(II), Ni(II), Co(II), Fe(III), and UO2(II) complexes of a new Schiff base hydrazine derived from 7-chloro-4-hydrazinoquinoline. Spectroc. Acta A **66**, 28–36 (2007)
10. S. Meghdadi, M. Amirnasr, K. Mereiter, H. Molaee, A. Amiri, Synthesis, structure and electrochemistry of Co(III) complexes with an unsymmetrical Schiff base ligand derived from 2-aminobenzylamine and pyrrole-2-carboxaldehyde. Polyhedron **30**, 1651–1656 (2011)
11. J. Losada, I.D. Peso, L. Beyer, Synthesis, electrochemical properties and electro-oxidative polymerization of copper(II) and nickel(II) complexes with N-benzoylthiourea ligands containing pyrrole groups. Transit. Met. Chem. **25**, 112–117 (2000)
12. A. Adhikari, S. Radhakrishnan, R. Patil, Influence of dopant ions on properties of conducting polypyrrole and its electrocatalytic activity towardsmethanol oxidation. Synth. Met. **159**, 1682–1688 (2009)
13. S. Bhunia, S. Koner, Heterogeneous catalyst (Tethering of nickel(II) Schiff-base complex onto mesoporous silica: an efficient heterogeneous catalyst for epoxidation of olefins. Polyhedron **30**, 1857–1864 (2011)
14. S.H. Kazemi, R. Mohamadia, Electrochemical fabrication of a novel conducting metallopolymer nanoparticles and its electrocatalytic application. Electrochim. Acta **109**, 823–827 (2013)
15. J. Losada, I. del Peso, L. Beyer, Journal of electroanalytical chemistry, redoxandelectrocatalytic properties of electrodes modified by films of polypyrrolenickel(II) Schiff-base complexes. J. Electroanal. Chem. **447**, 147–154 (1998)
16. A.G. Bernardo da Cruz, J.L. Wardell, V.D.M. Rangel, R.A. Simão, A.M. Rocco, Preparation and characterization of a polypyrrolehybridfilm with [Ni(dmit)2]2-, bis(1,3-dithiole-2-thione-4,5-dithiolate)nickellate(II). Synth. Met. **157**, 80–90 (2007)
17. C.S. Martin, T.R.L. Dadamos, M.F.S. Teixeira, Development of an electrochemical sensor for determination of dissolved oxygenby nickel–salen polymeric film modified electrode. Sens. Actuator B-Chem **175**, 111–117 (2012)
18. M.H. Mashhadizadeh, I. Sheikhshoaie, S. Saeid-Nia, Nickel(II)-selective membrane potentiometric sensor usinga recently synthesized Schiff base as neutral carrier. Sens. Actuators, B **94**, 241–246 (2003)
19. H.-G. Aslan, S. Özcan, N. Karacan, Synthesis, characterization and antimicrobial activity of salicylaldehydebenzenesulfonylhydrazone (Hsalbsmh)and its Nickel(II), Palladium(II), Platinum(II), Copper(II), Cobalt(II) complexes. Inorg. Chem. Comm. **14**, 1550–1553 (2011)
20. M. Rajasekar, S. Sreedaran, R. Prabu, V. Narayanan, R. Jegadeesh, N. Raaman, A.K. Rahiman, Synthesis, characterization, and antimicrobial activities of nickel (II) and copper(II) Schiff-base complexes. J. Coord. Chem. **63**, 136–146 (2010)
21. I.M. Mustafa, M.A. Hapipah, M.A. Abdull, T.R. Ward, Synthesis, structural characterization, and anti-ulcerogenic activity of Schiff base ligands derived from tryptamine and 5-chloro, 5-nitro, 3,5-ditertiarybutyl salicylaldehyde and their nickel(II), copper(II), and zinc(II) complexes. Polyhedron **28**, 3993–3998 (2009)
22. M.C. Burla, R. Caliandro, M. Camalli, B. Carrozzini, G.L. Cascarano, L. De Caro, C. Giacovazzo, G. Polidori, R. Spagna, An improved tool for crystal structure determination and refinement. J. Appl. Cryst. **38**, 381–388 (2003)
23. G.M. Sheldrick, A short history of SHELX. Acta. Cryst. A. **64**, 112–122 (2008)
24. L.J. Farrugia, WinGX and ORTEP for Windows: an update. J. Appl. Cryst. **45**, 849–854 (2012)

25. R.K. Parashar, R.C. Sharma, A. Kumar, G. Mohan, Stability studies in relation to IR data of some Schiff base complexes of transition metals and their biological and pharmacological studies. Inorg. Chim. Acta **151**, 201–208 (1988)
26. Y. Yang, Y. Zhang, S. Hao, J. Guan, H. Ding, F. Shang, P. Qiu, Q. Kan, Heterogenization of functionalized Cu(II) and VO(IV) Schiff base complexes by direct immobilization onto amino-modified SBA-15: styrene oxidation catalysts with enhanced reactivity. Appl. Catal. A: Gen. **381**, 274–281 (2010)
27. C. Rimington, Spectral-absorption coefficients of some porphyrins in the Soret-band region. J. Biochem. **75**, 620–623 (1960)
28. R.C. Felicio, G.A. Da Silva, L.F. Ceridorio, E.R. Dockal, Tetradentate Schiff Base Copper (II) Complexes. Synth. React. Met. Org. Chem. **29**, 171–192 (1999)
29. S.M. Abu-El-Wafa, R.M. Issa, C.A. McAuliffe, Unusual Cu(III)-Schiff'S Base complexes. Inorg. Chim. Acta **99**, 103–106 (1985)
30. R.J. Abraham, M. Mobli, R.J. Smith, ^{1}H chemical shifts in NMR: part 19^{+}. Carbonyl anisotropies and steric effects in aromatic aldehydes and ketones. Magn. Reson. Chem. **41**, 26–36 (2003)
31. A. Ourari, K. Ouari, W. Moumeni, L. Sibous, Unsymmetrical tetradentate Schiff base complexes derived from 2,3-diaminophenol and salicylaldehyde or 5-bromosalicylaldehyde. Trans. Met. Chem. **31**, 169–175 (2006)
32. P. Gili, M.G. Martin, Reyes, P. Martin Zarza, M.F.C. Guedes Da Silva, Y-Y. Tong, A.J.L. Pombeiro, Complexes of Mn(II) and Mn(III) with the Schiff base N-[2-(3-ethylindole)]pyridoxaldimine. Electrochemical study of these and related Ni(II) and Cu(II) complexes. Inorg. Chim. Acta **255**, 279–288 (1997)
33. M. Shebl, S.M.E. Khalil, S.A. Ahmed, H.A. Medien, Synthesis, spectroscopic characterization and antimicrobial activity of mono-, bi- and tri-nuclear metal complexes of a new Schiff base ligand. J. Mol. Struct. **980**, 39–50 (2010)
34. R.J. Platt, Classification of spectra of Cata-condensed hydrocarbons. J. Chem. Phys. **17**, 484–494 (1949)
35. R.M. Silverstein, G.C. Bassler, T.C. Morrill, *spectrometric identification of organic compounds*, 4th edn. (John Wiley and Sons, Hoboken, 1981), p. 196
36. S. Durmus, A. Atahan, M. Zengin, Synthesis, characterization and electrochemical behavior of some Ni(II), Cu(II), Co(II) and Cd(II) complexes of ONS type tridentate Schiff base ligand. Spectroc. Acta. A **84**, 1–5 (2011)
37. J.C. Liu, J. Cao, W.T. Deng, Hydrothermal synthesis, crystal structure and electrochemical properties of Cu(II) complex with 2-(1H-1,2,4-triazol-1-yl)acetic acid. Chin. J. Inorg. Chem. **26**, 343–346 (2010)
38. L.-Q. Chai, H.-S. Zhang, J.-J. Huang, Y.-L. Zhang, An unexpected Schiff base-type Ni(II) complex:synthesis, crystal structures, fluorescence, electrochemical property and SOD-like activities. Spectroc. Acta. A **137**, 1386–1425 (2014)
39. B.K. Singh, P. Mishra, A. Prakash, N. Bhojak, Spectroscopic, electrochemical and biological studies of the metal complexes of the Schiff base derived from pyrrole-2-carbaldehyde and ethylenediamine. Arab. J. Chem. **10**(007), 10–1016 (2012)
40. A. Anthonysamy, S. Balasubramanian, Synthesis, spectral, thermal and electrochemical studies of nickel (II) complexes with N2O2 donor ligands. Inorg. Chem. Commun. **8**, 908–911 (2005)
41. A.H. Kianfar, L. Keramat, M. Dostani, M. Shamsipur, M. Roushani, F. Nikpour, Synthesis, spectroscopy, electrochemistry and thermal study of Ni(II) and Cu(II) unsymmetrical N2O2 Schiff base complexes. Spectroc. Acta. A **77**, 424–429 (2010)
42. T.R.L. Dadamos, M.F.S. Teixeira, Electrochemical sensor for sulfite determination based on a nanostructured copper–salen film modified electrode. Electrochim. Acta **54**, 4552–4558 (2009)
43. M. Vilas-Boas, C. Freire, B. de Castro, A.R. Hillman, Electrochemical characterization of a novel salen-type modified electrode. J. Phys. Chem. **102**, 8533–8540 (1998)
44. P. Audebert, P. Hapiot, P. Capdevielle, M. Maumy, Electrochemical polymerization of several salen-type complexes. Kinetic studies in the microsecond time range. J. Electroanal. Chem. **338**, 269–278 (1992)
45. P. Audebert, P. Capdevielle, M. Maumy, Redox and conducting polymers based on salen-type metal units; electrochemical study and some characteristics. New J. Chem. **16**, 697–703 (1992)
46. P. Guo, T.-W. Hui, K.-C. Cheung, K.-Y. Wong, K.-K. Shiu, Charge propagation in nickel 6,6′-bis(2′-hydroxyphenyl)-2,2′-bipyridine polymer film doped with perchlorate anions. J. Electroanal. Chem. **498**, 142–151 (2001)

47. A. Ciszewski, I. Stepniak, Preparation, characterization and redox reactivity of glassy carbon electrode modified with organometallic complex of nickel. Electrochim. Acta **76**, 462–467 (2012)
48. M. Revenga-Parra, T. Garcıa, E. Lorenzo, F. Pariente, Electrocatalytic oxidation of methanol and other short chain aliphatic alcohols on glassy carbon electrodes modified with conductive films derived from NiII-(N, N_-bis(2,5-dihydroxybenzylidene)-1,2-diaminobenzene). Sens. Actuator B-Chem. **130**, 730–738 (2008)
49. A. Ourari, D. Aggoun, L. Ouahab, Poly(pyrrole) films efficiently electrodeposited using new monomersderived from 3-bromopropyl-N-pyrrol and dihydroxyacetophe none—Electrocatalytic reduction ability towards bromocyclopentane. Coll Surf. A Physicochem. Eng. Asp. **446**, 190–198 (2014)
50. M.S. Ureta-Zanartu, C. Berrios, J. Pavez, J. Zagal, C. Gutierrez, J.F. Marco, Electrooxidation of 2-chlorophenol on polyNiTSPc-modified glassy carbon electrodes. J. Electroanal. Chem. **553**, 147–156 (2003)